

May 22, 2024

## Luminescence dating report for Dr. Michael Polenz, from the Washington Geological Survey

ISGS code	Sample	Equivalent dose (Gy) <sup>1</sup>	Dose rate (Gy/ka)	Age (ka) <sup>1</sup>	n (accepted/total)
952	EVm051B	293 ± 31	2.79 ± 0.09	105 ± 12	8/10

<sup>1</sup> fading corrected (Huntley and Lamothe, 2001)

Optically stimulated luminescence (OSL) dating was measured on K-feldspar (150 – 250 µm), on small aliquots. The age was corrected for anomalous fading, by following an individual aliquot approach. Uncertainties are reported at a 1σ significance, providing a level of confidence of approximately 67%. The uncertainties combine random and systematic errors, added in quadrature. The beta dose rate on the luminescence system was calibrated against the Risø quartz calibration batch 90, and updated to the latest value (Autzen et al., 2022). Further details can be found in the report.



Sebastien Huot, Ph.D.

Illinois State Geological Survey

Champaign, Illinois

shuot@illinois.edu

+1-217-300-2579 (office)

This is a report on the optically stimulated luminescence (IRSL) dating of a single sample delivered to us by Dr. Michael Polenz, during Summer 2023. The sample was retrieved in an opaque tube, from a natural outcrop. The depositional environment is interpreted as fluvial or glaciofluvial. For the purposes of internal identification, we labeled this sample ISGS 952.

## 1. Sample preparation and equipment

The tube was opened and the mineral extraction was conducted in a subdued orange light environment. One inch of sediment (i.e. the external portion) was removed from both ends of each tube because these might have been partially exposed to light during sampling. Sediment from the external portions was used to measure the in situ water content and its radioactive content (uranium, thorium, and potassium), both for dose rate calculation. These minerals were wet sieved to retrieve the 150- to 250- $\mu\text{m}$  grain size. A hydrochloric acid attack (HCl, 10%) was applied to dissolve any carbonate minerals that might be present. Using a heavy liquid solution (2.58 g/mL) of lithium heteropolytungstate (LST), we separated K-feldspar (<2.58) from the quartz and Na-feldspar minerals (>2.58). There was an unusually large amount of low density minerals. The initial luminescence signal observed from these K-feldspar minerals were unusually dim. To further increase the purity of these K-feldspar, we made use of a Frantz magnetic separator and relied on the non-magnetic fraction (0.7 ampere) for IRSL dating. A lot of minerals had a paramagnetic property. Personal experience has shown me that these paramagnetic minerals, contaminating the K-feldspar low density fraction do not emit any luminescence signal. These purified K-feldspar grains displayed a bright luminescence signal, as is typical.

The beta dose rate on the luminescence system was calibrated against the Risø quartz calibration batch 90, and was updated to the latest value (Autzen et al., 2022). Please note that Risø has refined the calculated value, attributed to their quartz calibration, by further constraining the systematic uncertainties, inherent to that process. This results in a calculated OSL/IRSL age increase by 8.25 %. This retrospectively affects all luminescence ages, measured since the year 2000, from every luminescence dating laboratories around the world that relies on the Risø quartz calibration (batch 1 through 125).

To obtain the dose rate, sediments from the external portion of each sampling tube were dried, and a representative portion was encapsulated in thin disk-shaped containers (~20 g) and sealed with 2 layers of epoxy gel. A minimum waiting time of 21 days after sealing is recommended to restore the radioactive equilibrium of radon-222 daughter products (Gilmore, 2008). The specific activities (Bq/kg) were measured with a broad-energy high-purity germanium detector (BEGe), in a planar configuration, shielded by 15 cm of lead. Efficiency calibration of the detector was obtained with a set of six certified standards (IAEA-RGU-1, IAEA-RGTh-1, IAEA-RGK-1, IAEA-385, NIST 4350b, and NIST 4355).

## 2. Equivalent dose (De) measurements

For the equivalent doses (De) measurements, we relied on an automated Risø TL-DA-20 system, equipped with a set of blue (470 nm) and infrared (870 nm) LEDs, for light stimulation. Detection was made in the blue (combination of Schott BG39 and Corning 7-59 glass filters) for K-feldspar. For each sample, we dispensed K-feldspar grains over a small area (2 mm), onto a silicon oil covered stainless disk (10 mm diameter). Around 20 - 50 grains were dispensed on each disks' center. Several aliquots were measured, for each sample.

IRSL measurements were carried out with a single-aliquot regenerative dose (SAR) protocol (Table 1). The optimal measurement parameters were selected by a dose recovery test (latent dose bleached with sunlight for 1 day). An initial dose was given at first (that was a close match to the measured equivalent dose for each sample; 250 Gy) and it was subsequently recovered by measuring its equivalent dose with the SAR protocol. The samples responded reasonably well to the treatment. From this we selected a preheat temperature (Lx and Tx) of 250°C (held for 60 seconds; Huot and Lamothe, 2003). The dose recovery test was performed for every sample using the most appropriate temperature. It yielded an average measured-to-given dose ratio of  $0.92 \pm 0.03$ . This outcome is positive. Considering this result, we opted to select the parameters in Table 1.

**Table 1.** Measurement steps for the single-aliquot regenerative protocol (Huot and Lamothe, 2003; Murray and Wintle, 2000)

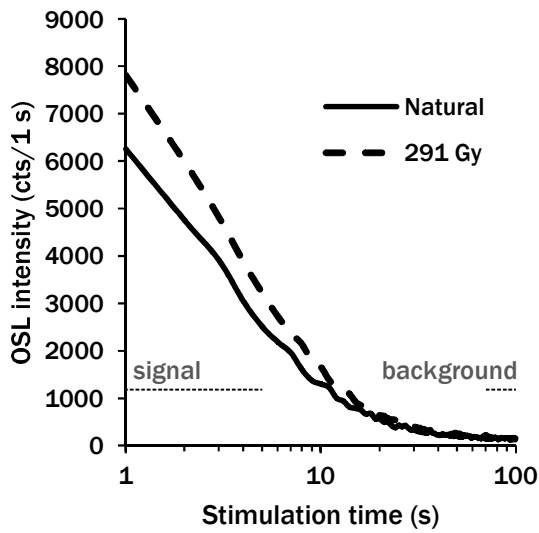
Step	Procedure (K-feldspar)
1	Regeneration <sup>1</sup> /natural dose
2	Preheat (250 °C), hold for 60 seconds
3	Pause <sup>2</sup>
4	IRSL stimulation with IR LEDs at 50 °C for 100 seconds (Lx)
5	Test dose beta irradiation (145 or 58 Gy)
6	Preheat (250 °C) for 60 seconds
7	IRSL stimulation with IR LEDs at 50 °C for 100 seconds (Tx)
8	Repeat Steps 1–7 with further regeneration doses

<sup>1</sup> For equivalent dose measurements, we gave a range of laboratory-induced doses that would properly encompass the variability of the observed natural luminescence.

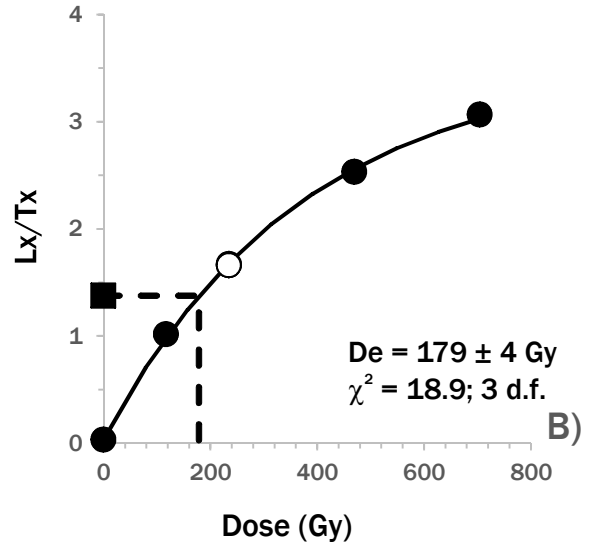
<sup>2</sup> There was no pause for equivalent dose measurements. A pause was observed here for anomalous fading measurements.

### 2.1 Equivalent dose calculation

For the equivalent dose, all calculations were made using the “late light” approach for background subtractions, by taking the initial 5 data channels (5 seconds) from the IRSL decay curve and removing the background from the end of the stimulation curve (30 data channels, 30 seconds; Figure 1a).



A)



B)

Figure 1a. Typically IRSL decay curve, for a naturally dose aliquot (solid curve) or laboratory-induced dose (dashed curve, in Gy). The area under the curve is proportional to the dose of radiation stored within the mineral. Their luminescence growth curve and fading rate are shown in Figure 1b and 2. Note the logarithmic time axis.

Figure 1b. Luminescence dose response curve for the same aliquots shown in Figure 1a. Each point corresponds to the OSL ( $L_x$ ; measurement step 4 in Table 1) of a natural (square) or laboratory-induced dose (filled circles)), normalized by the luminescence response to a fixed test dose ( $T_x$ ; measurement step 7). A repeat measurement (the recycling test; open circles) was performed at the end. The equivalent dose is obtained by interpolation. For the aliquot shown here, the observed measurements scatter well around the predicted best-fit curve.

Uncertainties relied on Poisson statistics. For curve fitting, we also propagated the uncertainties from the optimized luminescence growth curve parameters. In addition, when the observed scatter about the best fit regression line was too high, the uncertainties were increased (Figure 1b). For this, we relied on the one-tailed probability  $\chi^2$  distribution, with  $N - 3$  degrees of freedom (where  $N$  is the number of measured data points). When the probability was lower than 15% (i.e., the data points scattered above and beyond the best fit line), the uncertainties for the optimized parameters were expanded by Student's  $t$  values for  $N - 3$  degrees of freedom (Brooks et al., 1972; Ludwig, 2003).

## 2.2. Anomalous fading

The luminescence of feldspar is known to underestimate the 'true' burial age, typically by about 30 to 50 % (Aitken, 1998). The cause is known to us: anomalous fading (Wintle, 1973). Luminescence dating is akin to a filling a glass with water. At time zero, the glass is empty (i.e. the zeroing effect of sunlight). You pour water into it, at a constant rate (dose rate), but stop before reaching the top (sampling). The volume of water contained in the glass represents the equivalent dose in luminescence (the total amount of radiation energy trapped by the mineral during burial). By dividing the volume (equivalent dose) by the rating of water filling (dose rate), we can calculate when was the glass empty (length of burial).

Now, what if there is a very small hole in the glass. As you pour water into it, you lose water through that hole, at a steady rate. Now, the volume of water that remains in the glass underestimates the real amount of water that was poured in it. If you can measure the size of the hole, it is possible to calculate what would have been the real amount of water contained in the glass.

The luminescence of quartz (our workhorse in luminescence dating) is akin to a perfect glass, whereas K-feldspar is that of a glass with a hole. At the time this phenomenon was first described in feldspar, the mechanism underlying that lost, or fading, was unknown to us; hence, it was termed 'anomalous fading'. It was 'anomalous' because from thermodynamic principles, it is expected that a trapped electron would remain so for many millions of years (i.e. water can evaporate from your glass) at room temperature (i.e. just like water, where the evaporation rate is temperature dependent, so is the thermal lifetime of a trapped electron). Yet, trapped elections in feldspar are leaking faster than they should and that rate of leakage is independent of temperature. Hence, anomalous!

Nowadays, we know how to deal with it. We know how to measure the size of the hole (fading rate; Auclair et al., 2003) and we know how to properly correct for it (e.g. Huntley and Lamothe, 2001). We acknowledge that a novel measurement technique to minimize, and sometimes circumvent, the IRSL age underestimation from anomalous fading has emerged in the literature (post-IR IRSL; Buylaert et al., 2012). An attempt was made for this sample; unfortunately, it yielded a very low

luminescence intensity. Therefore, we opted to retain the < old school > method (i.e. IRSL 50 °C) of measuring and correcting for fading.

### 2.3 Fading corrected age

Measured IRSL ages were corrected for anomalous fading using the Huntley and Lamothe (2001). The fading rate was measured for each equivalent dose, aliquot by aliquot. After the equivalent dose measurement, the aliquots were bleached under normal sunlight, for one day. After, the anomalous fading measurement was initiated, using the same measurement parameters (Table 1). Thus, pairing equivalent dose with anomalous fading rate, aliquot by aliquot. The laboratory-induced dose (step 1) was fixed, at 145 Gy, along with a test dose (step 5) of 58 Gy. Also, there was a 'pause' in effect, at step 3, which ranged from 20 minutes up to 25 hours (Figure 2; Auclair et al., 2003).

The < as measured > equivalent dose from each aliquot was corrected with the aid of the Huntley and Lamothe (2001) model. This has a limitation: it is accurate, as long as the equivalent dose is within the linear approximation of the luminescence growth curve. For these samples, the luminescence growth curve can be approximated to a simple straight line for radiation doses easily up to 200 Gy, and more (Figure 1b). For sample EVm051B, this is well within the range of its measured equivalent dose. The anomalous fading correction model may still provide reliable ages (Buylaert et al., 2008). Over the years, this model has proven to be highly successful in yielding accurate ages, whenever an independent assessment could be made.

### 2.4 Age distribution

A weighted average (using the central age model; Galbraith et al., 1999) was used in all calculations, except when noted otherwise. The central age model provides an overdispersion parameter. This parameter characterizes the degree to which the observed weighted distribution is consistent with the predicted weighted distribution from the observed data. At 0%, the observed distribution is equal to the statistical prediction. In luminescence dating, it is common for the observed distribution to be slightly larger than the expected distribution by a value of approximately 20%. This means that the calculated uncertainties tend to underestimate the "real" uncertainties because of intrinsic (e.g., instrumental uncertainties, luminescence characteristics of quartz and K-feldspar) or extrinsic (e.g., partial bleaching, external beta microdosimetry) factors. The central age model expands the age uncertainty in an attempt to account for this discrepancy. Here, the overdispersion is within the normality (Table 2, Figure 3). The fading corrected age is presented in Table 3.

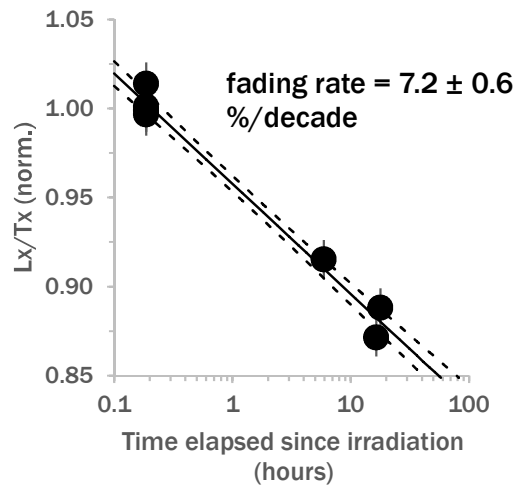


Figure 2. Anomalous fading measurement, for a representative aliquot of each sample (the same shown in Figure 1a and 1b). Repeated measurement cycles are made, on the same aliquot, with different delays between the irradiation and the IRSL measurement (i.e. step 3 from Table 1). The slope is proportional to the fading rate, used in the fading correction model. The 2 dashed lines represent the  $1\sigma$  error envelopes. Note the logarithmic time axis.

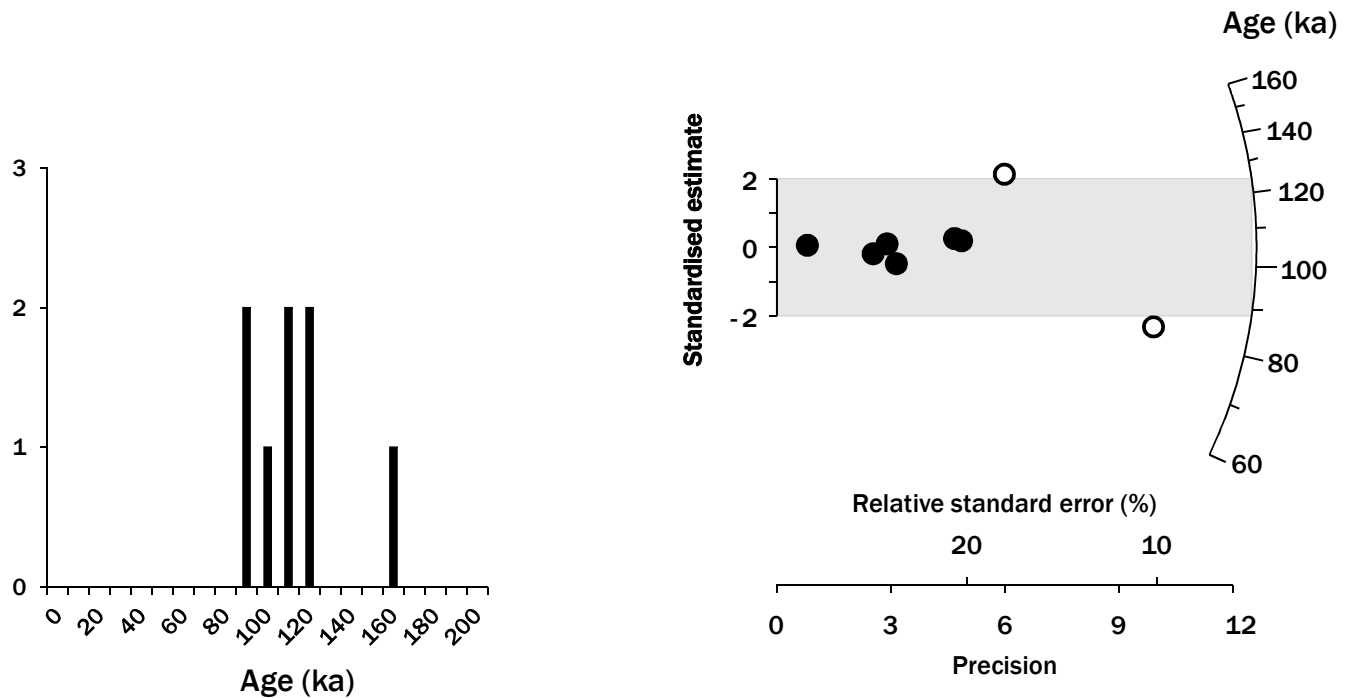


Figure 3. Age distributions, as a histogram and a radial plot, for all samples. Each circle on the radial plot represents the age and uncertainty, for a single aliquot. The age is read on the arc axis, by drawing a straight line from (0, 0), passing through a circle and intersecting the radial axis (log scale). The (0, 0) coordinate corresponds to a 0 standardised estimate (y-axis) and 0 precision (x-axis). The uncertainty is read on the horizontal axis, by drawing a perpendicular line reaching a circle. Hence, two aliquots, having the same age, but with different uncertainty, will lay on the same straight line (from (0, 0) to the radial axis). The aliquot with the smaller uncertainty (higher precision) will be closer to the arc. Values (filled circles) within the light grey shaded band are consistent (at  $2\sigma$ ) with the weighted mean (Central Age Model). A cluster of aliquots within this shaded band expresses confidence that we have a population of grains consistent with a single age.

Table 2. Age overdispersion parameters<sup>1</sup>

ISGS code	Sample	Overdispersion (%)
952	EVm051B	19 ± 10

<sup>1</sup>A value of 20% is typical in luminescence

Table 3. Measured versus corrected ages

ISGS code	sample	equivalent dose (Gy)	age (ka)	fading corrected age (ka)	average fading rate (%/decade)
952	EVm051B	215 ± 9	77 ± 5	105 ± 12	4.9 ± 1.0

### 3. Dose rate

The water content was measured for each sample. The as-received water content was relatively humid (Table 4). It seems reasonable, given the location of this deposit. We expect this state would have held, for most of the sediments' burial history. Given this, we opted for the values presented in the table.

We assigned a water content uncertainty of 5 % to account for possible variation during the entire length of burial. The bulk density was measured for this sample, providing a value of 1.45 g/cm<sup>3</sup>.

Table 4. Water content, measured from the sample, with the value presumed to have prevailed during the burial, along with sediment density.

ISGS code	Sample	in situ (%)	presumed (%)	density (g/cm <sup>3</sup> )
952	EVm051B	13 – 17	15 ± 5	1.45

Waiting times of around 30 days were observed before measuring the radioactive activities of uranium, thorium, and potassium, from which we can derive contributions from alpha, beta, and gamma energy decay (Table 5).



Table 5. Specific activity (Bq/kg)

ISGS code	Sample	<sup>238</sup> U	<sup>226</sup> Ra	<sup>210</sup> Pb	<sup>232</sup> Th	<sup>40</sup> K
952	EVm051B	23.0 ± 1.5	22.3 ± 0.4	21.3 ± 1.6	22.7 ± 0.4	403 ± 8

For K-feldspar, we assumed an internal content of  $12.5 \pm 0.5$  % and  $400 \pm 100$  ppm, for potassium and rubidium, respectively (Huntley and Baril, 1997; Huntley and Hancock, 2001). A conservative  $0.10 \pm 0.05$  “a value” (efficiency of alpha particles compared with beta particles upon inducing a trapped charge in quartz and feldspar; i.e., alpha is only 10% as effective as beta) was retained (Table 6).

Table 6. Contribution to the dose rate, expressed in Gy/ka<sup>1</sup>

ISGS code	beta external (Gy/ka)	gamma (Gy/ka)	cosmic ray (Gy/ka)	depth (m)	water (%)	total (Gy/ka)
952	1.09 ± 0.07	0.67 ± 0.02	0.15 ± 0.01	4	15 ± 5	2.79 ± 0.09

<sup>1</sup> For K-feldspar minerals, we relied on an external alpha and internal beta dose rate contributions of  $0.064 \pm 0.038$  and  $1.091 \pm 0.074$  Gy/ka, respectively.

#### 4. Uncertainty budget

The breakdown of the uncertainties, between the total random and systematic sources, are presented in table 7. The random uncertainties reflect the standard error on the best estimate (i.e. from the central age model) for the equivalent dose (in seconds of laboratory-induced irradiation). The systematic uncertainties reflect here the combined (in quadrature) components of the environmental dose rate and calibration of the beta source on the luminescence system.

Table 7. Random and systematic uncertainties (in years), at 1 sigma

ISGS code	Sample	Age (ka)	1σ (random)	1σ (systematic)
952	EVm051B	104.948 ± 11.847	± 10.992	± 4.417

## 5. Conclusion

In summary, the luminescence properties of these K-feldspar minerals behaved reasonably well, as we routinely expect from these minerals. Anomalous fading was measured and corrected with a single aliquot approach. The sample appears to have been well-bleached at deposition.

Sebastien Huot, PhD

Illinois State Geological Survey

## References

- Aitken, M.J., 1998. An introduction to optical dating. Oxford University Press, Oxford.
- Auclair, M., Lamothe, M., Huot, S., 2003. Measurement of anomalous fading for feldspar IRSL using SAR. *Radiation Measurements* 37, 487-492.
- Autzen, M., Andersen, C.E., Bailey, M., Murray, A.S., 2022. Calibration quartz: An update on dose calculations for luminescence dating. *Radiation Measurements* 157, 106828.
- Brooks, C., Hart, S.R., Wendt, I., 1972. Realistic use of two-error regression treatments as applied to rubidium-strontium data. *Reviews of Geophysics* 10, 551-577.
- Buylaert, J.-P., Jain, M., Murray, A.S., Thomsen, K.J., Thiel, C., Sohbat, R., 2012. A robust feldspar luminescence dating method for Middle and Late Pleistocene sediments. *Boreas* 41, 435-451.
- Buylaert, J.P., Murray, A.S., Huot, S., 2008. Optical dating of an Eemian site in Northern Russia using K-feldspar. *Radiation Measurements* 43, 715-720.
- Galbraith, R.F., Roberts, R.G., Laslett, G.M., Yoshida, H., Olley, J.M., 1999. Optical dating of single and multiple grains of quartz from Jinmium rock shelter, northern Australia: part I, experimental design and statistical models. *Archaeometry* 41, 339-364.
- Gilmore, G.R., 2008. Practical gamma-ray spectrometry, 2nd ed. John Wiley & Sons, Ltd.
- Huntley, D.J., Baril, M.R., 1997. The K content of the K-feldspars being measured in optical dating or in thermoluminescence dating. *Ancient TL* 15, 11-13.
- Huntley, D.J., Hancock, R.G.V., 2001. The Rb contents of the K-feldspar grains being measured in optical dating. *Ancient TL* 19, 43-46.
- Huntley, D.J., Lamothe, M., 2001. Ubiquity of anomalous fading in K-feldspars and the measurement and correction for it in optical dating. *Canadian Journal of Earth Sciences* 38, 1093-1106.
- Huot, S., Lamothe, M., 2003. Variability of infrared stimulated luminescence properties from fractured feldspar grains. *Radiation Measurements* 37, 499-503.
- Ludwig, K.R., 2003. Mathematical-statistical treatment of data and errors for Th-230/U geochronology, in: Bourdon, B., Henderson, G.M., Lundstrom, C.C., Turner, S.P. (Eds.), *Uranium-Series Geochemistry*. Mineralogical Society of America, pp. 631-656.
- Murray, A.S., Wintle, A.G., 2000. Luminescence dating of quartz using an improved single-aliquot regenerative-dose protocol. *Radiation Measurements* 32, 57-73.
- Wintle, A.G., 1973. Anomalous fading of thermoluminescence in mineral samples. *Nature* 245, 143-144.